Measurements of Circular Depolarization Ratio with the Radar with Simultaneous Transmission / Reception

Alexander Ryzhkov[1,2], Pengfei Zhang[1,2], Qing Cao[3], Sergey Matrosov[4,5], Valery Melnikov[1,2], and Michael Knight[3]

[1]*Cooperative Institute for Mesoscale Metorological Studiest,University of Oklhoma, Norman, USA*
[2]*NOAA/OAR/National Severe Storms Laboratory, Norman, USA*
[3]*Enetrprise Electroniscs Corporation, Enterprise, Alabama, USA*
[4]*Coopertaive Instiitute for Research in Environmental Sciences, University of Colorado at Boulder, Boulder, Colorado, USA*
[5]*NOAA/OAR/Earth Systems Research Laboratory, Boulder, Colorado, USA*

(Dated: 13 July 2014)

1 Introduction

Circular depolarization ratio (CDR) is a polarimetric variable which was historically among the first measured by dual-polarization weather radars transmitting and receiving waves with circular polarization. One of its advantages is that it is primarily determined by the shape and phase composition of atmospheric particles and weakly depends on particle orientation as opposed to linear depolarization ratio (LDR) which is also considerably lower than CDR and difficult to measure for low signal-to-noise ratio. It was shown in the series of studies by Matrosov et al. (2001, 2012) that the CDR dependency on antenna elevation angle can be used to distinguish between planar and columnar types of crystals in the ice parts of clouds.

One of the drawbacks of the "classical" CDR is that it is heavily biased by propagation effects and differential phase in particular which precluded its operational utilization so far (Al-Jumily et al. 1991; Torlaschi and Holt 1993, 1998). This was one of the reasons why the choice of operational polarimetric radar was made in favor of the radar with simultaneous transmission / reception which measures differential reflectivity Z_{DR}, differential phase Φ_{DP}, cross-correlation coefficient ρ_{hv} but not CDR.

Matrosov (2004) was the first who proposed the idea of measuring CDR by the radar with simultaneous transmission / reception operating at X band. In this study, we further explore such an approach and demonstrate how CDR can be obtained by operational dual-polarization radars along with traditionally measured Z_{DR}, Φ_{DP}, and ρ_{hv} without slowing down or compromising the standard mode of operation. Moreover, our method automatically eliminates the impact of propagation effects on CDR at the signal processor level. This, however, requires control of system differential phase on transmission $\Phi_{DP}^{(t)}$ using high-power phase shifter to ensure that the polarization state of transmitted wave is close to circular. Polarimetric C-band radar with such configuration was built by the Enterprise Electronics Corporation and some examples of CDR data will be presented herein.

2 Theoretical background

Circular depolarization ratio CDR can be estimated from differential reflectivity Z_{DR}, linear depolarization ratio LDR, cross-correlation coefficient ρ_{hv}, and differential phase Φ_{DP} measured in a linear horizontal – vertical polarization basis using the formula (Matrosov 2004)

$$C_{dr} = \frac{<|S_{hh}\exp(-j\Phi_{DP}) \pm 2jS_{hv}\exp(-j\Phi_{DP}/2) - S_{vv}|^2>}{<|S_{hh}\exp(-j\Phi_{DP}) + S_{vv}|^2>} \tag{1}$$

$$CDR = 10\log(C_{dr})$$

where S_{ij} are elements of the scattering matrix of hydrometeors. It can be easily shown that if the mean canting angle of hydrometeors is equal to zero then

$$C_{dr} = \frac{1 + Z_{dr}^{-1} - 2\rho_{hv}Z_{dr}^{-1/2}\cos(\Phi_{DP}) + 4L_{dr}}{1 + Z_{dr}^{-1} + 2\rho_{hv}Z_{dr}^{-1/2}\cos(\Phi_{DP})} \tag{2}$$

In (2), Z_{dr} and L_{dr} are differential reflectivity and linear depolarization ratio expressed in linear units. One of the serious problems with circular depolarization ratio CDR is that it is strongly affected by propagation effects and differential phase shift in particular. Correction of CDR for differential phase is a big challenge which is one of the reasons why CDR has never been used for operational meteorological applications despite its attractiveness compared to linear depolarization ratio LDR which is weakly affected by propagation effects but, as opposed to CDR, strongly depends on the particle orientations. We are suggesting a novel technique which allows to measure CDR in the standard SHV mode of radar operations and effectively eliminates the dependency of estimated CDR on differential phase.

The complex voltages of received signals in the two orthogonal channels in the case of simultaneous transmission / reception of the H and V waves are

$$V_h = C\{S_{hh}\exp\{-j(\Phi_{DP}+\Phi_{DP}^{(t)}+\Phi_{DP}^{(r)})\} + S_{hv}\exp[-j(\Phi_{DP}/2+\Phi_{DP}^{(r)})]\} \quad (3)$$
$$V_v = C\{S_{hv}\exp[-j(\Phi_{DP}/2+\Phi_{DP}^{(t)})] + S_{vv}\}$$

Herein, Φ_{DP} is propagation phase in the atmosphere and $\Phi_{DP}^{(t)}$ and $\Phi_{DP}^{(r)}$ are system differential phases on transmission and reception respectively. Their sum is total system differential phase $\Phi_{DP}^{(sys)}$. The ratio

$$S_{dr} = \frac{<|V_h\exp[j(\Phi_{DP}+\Phi_{DP}^{(sys)})]-V_v|^2>}{<|V_h\exp[j(\Phi_{DP}+\Phi_{DP}^{(sys)})]+V_v|^2>} = \frac{\frac{1}{M}\sum_{m=1}^{M}|V_h(m)\exp[j(\Phi_{DP}+\Phi_{DP}^{(sys)})]-V_v(m)|^2}{\frac{1}{M}\sum_{m=1}^{M}|V_h(m)\exp[j(\Phi_{DP}+\Phi_{DP}^{(sys)})]+V_v(m)|^2} \quad (4)$$

where M is a number of radar samples accurately approximates intrinsic C_{dr} which is not biased by propagation effects provided that the system differential phase on transmission $\Phi_{DP}^{(t)}$ is close to 90°, i.e., the polarization of transmitted wave is close to circular. Implementation of this scheme requires utilization of high-power phase shifter to control $\Phi_{DP}^{(t)}$.

The equation for S_{dr} can be expanded as

$$S_{dr} = \frac{1+Z_{dr}^{-1}-2\rho_{hv}Z_{dr}^{-1/2}+4L_{dr}\sin^2(\Phi_{DP}/2+\Phi_{DP}^{(t)})}{1+Z_{dr}^{-1}+2\rho_{hv}Z_{dr}^{-1/2}+4L_{dr}\cos^2(\Phi_{DP}/2+\Phi_{DP}^{(t)})} \quad (5)$$

Depolarization ratio S_{dr} still depends on Φ_{DP} but such dependence is much weaker than the one described by Eq (2). For example, if $\Phi_{DP} = 0$ and $\Phi_{DP}^{(t)} = \pi/2$ then D_{dr} is exactly equal to C_{dr}.

The expression for D_{dr} can be written as

$$D_{dr} = \frac{P_h + P_v - 2\,\mathrm{Re}\{R_{hv}\exp[-j(\Phi_{DP}+\Phi_{DP}^{(sys)})]\}}{P_h + P_v + 2\,\mathrm{Re}\{R_{hv}\exp[-j(\Phi_{DP}+\Phi_{DP}^{(sys)})]\}} \quad (6)$$

In (6),

$$P_h = \frac{1}{M}\sum_{m=1}^{M}|V_h(m)|^2 \quad (7)$$

is a power of a horizontally polarized component of the radar return,

$$P_v = \frac{1}{M}\sum_{m=1}^{M}|V_v(m)|^2 \quad (8)$$

is a power of a vertically polarized component of the radar return, and

$$R_{hv} = \frac{1}{M}\sum_{m=1}^{M}V_h^*(m)V_v(m) \quad (9)$$

is a complex covariance which has its phase equal to the estimate of differential phase so that

$$R_{hv} = |R_{hv}|\exp[j(\Phi_{DP}+\Phi_{DP}^{(sys)})] \quad (10)$$

Substituting R_{hv} from (10) into (6) yields

$$D_{dr} = \frac{P_h + P_v - 2|R_{hv}|}{P_h + P_v + 2|R_{hv}|} \quad (11)$$

This means that CDR can be estimated using the combination of powers of the reflected signals at horizontal and vertical polarizations and the *magnitude* of the complex covariance R_{hv}. All three parameters are routinely calculated at each range gate in standard data processors for polarimetric radars and estimation of CDR from (11) is very simple and straightforward. Note that CDR = 10 log(S_{dr}) approximates "true" CDR quite well only if the differential phase on transmission is close to 90° which requires the use of a high-power phase shifter in one of the orthogonal channels.

As follows from (3), P_h, P_v, and R_{hv} slightly depend on the differential phase on transmission $\Phi_{DP}^{(t)}$ due to inherent cross-coupling of the H and V radar returns in the SHV mode of operation. Although the impact of $\Phi_{DP}^{(t)}$ on each of these variables is small, its influence on the numerator in (11) is quite substantial which dictates the need to control $\Phi_{DP}^{(t)}$ to obtain more accurate estimate of CDR.

3 Simulations based on real data

The circular depolarization ratio can be computed from the measurements of Z_{DR}, ρ_{hv}, and Φ_{DP} only if LDR is also available (which is not the case for operational polarimetric weather radars). For this purpose, we resort to the research data collected by the NCAR SPOL polarimetric radar which measured all needed variables. A thunderstorm case in Florida on 08/14/1998 is selected for analysis. This case is examined in the paper by Ryzhkov et al. (2002).

An example of vertical cross-sections of the measured Z, Z_{DR}, ρ_{hv}, LDR, Φ_{DP} as well as two estimates of CDR is displayed in Fig. 1. The first estimate of CDR (marked as "before correction") is obtained from Eq (2) and represents what would be measured by "true" circularly polarized radar. The impact of propagation (or Φ_{DP}) on CDR is obvious: CDR is grossly overestimated in the areas with even modest Φ_{DP} (up to 10 - 20°). Such on overestimation is expected to be much more dramatic at shorter radar wavelengths where Φ_{DP} is higher. Different approaches for correcting CDR for differential phase shift were discussed in literature (e.g., Torlaschi and Holt 1993, 1998) but none of them proved to be efficient.

The second estimate of CDR is obtained using D_{dr} as its proxy assuming $\Phi_{DP}^{(t)} = \pi/2$ in Eq (5). It is marked as CDR "after correction" and is not affected by propagation while being very consistent with the results of direct measurements of CDR and its theoretical simulations which can be found in literature (Jameson 1987; Al-Jumily et al. 1991; Torlaschi and Holt 1993,1998; Holt et al. 1999; Matrosov et al. 2001, 2012). It seems that corrected CDR is more informative above the melting layer than traditionally utilized Z_{DR} and ρ_{hv} and can complement other polarimetric measurements. CDR is 3 – 15 dB higher than LDR as their difference in the right bottom panel in Fig. 1 shows and, therefore, can be more reliably measured in the areas of weaker echo.

The plot of corrected CDR displayed in Fig. 1 is presented for the case when the polarization of transmitted wave is circular ($\Phi_{DP}^{(t)} = 90°$). We examined the influence of $\Phi_{DP}^{(t)}$ on the estimated CDR and compare the CDR cross-sections with $\Phi_{DP}^{(t)}$ changing from 90° to 20° (Fig. 2). The RHIs of CDR do not change significantly if $\Phi_{DP}^{(t)}$ is within 20 – 30° from its optimal value of 90°. This allows to substantially relax the requirements for calibration of the phase shifter.

In the previous example, CDR was computed from the radar moments (i.e., Z_{DR}, ρ_{hv}, LDR, and Φ_{DP}). In the next example, CDR is estimated directly from I and Q data collected by the polarimetric S-band KOUN WSR-88D radar in Norman, Oklahoma, as prescribed by formula (11). Fig. 3 shows composite RHI of the Z, Z_{DR}, Φ_{DP}, LDR, and CDR (biased and unbiased by propagation) for the storm observed on 07/03/2007. Z, Z_{DR}, Φ_{DP}, and CDR are estimated in the SHV mode of operation while LDR is measured in the LDR mode when only H wave is transmitted. The system differential phase on transmission $\Phi_{DP}^{(t)}$ was about 82° at the time of measurements. This means that polarization of transmitted wave in the SHV mode was very close to circular. Again, CDR estimated from Eq (11) does not exhibit bias attributed to differential phase.

4 Direct measurements of CDR with a prototype of operational radar

The suggested methodology for CDR measurements prescribing the use of high-power phase shifter and signal processing according to Eqs. (7) – (11) has been implemented by the Enterprise Electronics Corporation on its C-band dual-polarization radar with simultaneous transmission / reception at Enterprise, AL. Fig. 4 illustrates the field of CDR obtained simultaneously with Z, Z_{DR}, ρ_{hv}, and Φ_{DP} at elevation 4.5° during the stratiform rain event on 28 January 2014. CDR is displayed only in the areas of SNR > 20 dB. Circular depolarization ratio exhibits obvious enhancement in the melting layer and is consistent with other polarimetric radar variables.

The quality of CDR measurements can be evaluated using the expected consistency between CDR and Z_{DR} in pure rain. Fig. 5 shows that the scatterplot of CDR vs Z_{DR} in rain (right panel) where SNR > 20 dB corresponds very well to what is predicted at C band by theoretical simulations using large disdrometer dataset assuming that the width of the canting angle distribution is 10° (left panel).

Average vertical profiles of CDR, Z, Φ_{DP}, and ρ_{hv} obtained via azimuthal averaging of these variables at elevation 4.5° are shown in Fig. 6. The measured CDR is higher in the frozen part of the stratiform cloud than in rain below the melting layer which corresponds to the results of CDR measurements performed in the past studies which used "true" radars with circular polarization. This is a good indication that the C-band Sidpol radar in Enterprise, AL measures circular depolarization ratio with reasonably good accuracy.

5 Potential practical utilization of CDR

CDR does not have much additional value beyond what is available from Z, Z_{DR}, K_{DP}, and ρ_{hv} in warm parts of storms below the melting layer. It can be shown that CDR is well correlated with Z_{DR} in pure rain, and therefore does not provide supplemental information. In pure rain, CDR usually varies between -25 and -15 dB. However, CDR can contribute significantly to interpretation of polarimetric radar data above the melting layer. Three major challenging practical tasks can be addressed using CDR measurements: (1) detection of hail and determination of its size above the melting layer, (2) differentiating between various habits of ice aloft, and (3) quantification of riming which is associated with the presence of supercooled cloud water and signifies possible icing hazard to aircraft.

The Hail Size Discrimination Algorithm (HSDA) recently developed at NSSL (Ryzhkov et al. 2013b) capitalizes primarily on polarimetric signatures below the melting layer where melting hail is mixed with rain. This implies that hail has already been formed aloft and falls to the ground. For hail nowcasting and suppression it is more important to detect large hail earlier when it is just formed in the upper part of the storm where differential reflectivity which is the major informative parameter near the ground provides very little information about hail size. Indeed, Z_{DR} is close to zero in hail-bearing storms above the freezing level. In contrast, CDR above the freezing level varies significantly depending on hail size. Our simulations of CDR based on the microphysical model of hail described in Ryzhkov et al. (2013a) show that CDR can increase 10 – 15 dB if maximal hail diameter changes from 8 mm to 50 mm. Steady increase of CDR with maximal hail size is caused by progressively stronger resonance scattering effects for larger hailstones and decrease of the slope of the exponential size distribution in the case of larger hail.

Matrosov et al. (2001, 2012) showed that absolute values of CDR at grazing angles of antenna and its elevation dependence can be used for discrimination between different ice habits in the clouds. CDR significantly increases with decreasing antenna elevation for oblate types of snow crystals (hexagonal plates, thick plates, dendrites), whereas the elevation dependency of CDR is relatively "flat" for prolate type of crystals (columns, needles, etc.). At low elevation angles, CDR varies tremendously (from -30 dB to – 8 dB) depending on the ice habit. According to radar observations by Matrosov et al. (2001, 2012), pristine dendrites and hexagonal plates have highest values of CDR up to -8 dB followed by columns and aggregates of dendrites (-23 - -17 dB) with graupel indicating lowest CDR below -26 dB.

Riming is the process of freezing of small supercooled liquid droplets (with size of microns or tens of microns) on falling ice crystals and snowflakes. Supercooled liquid water can not be observed directly by weather surveillance radars because of small size of liquid droplets but its presence can be detected by estimating the degree of riming of ice crystals Riming tends to increase density and aspect ratio of ice particles, i.e., it makes them denser and more spherical. The density effect increases CDR while the shape effect changes CDR in the opposite direction. Both theoretical and experimental studies indicate that the effect of shape definitely prevails so that riming causes reduction in CDR. For a given snow habit, the change of aspect ratio due to riming can be quantified using the relation between rimed mass fraction and the degree of riming r (Mosimann et al. 1994)

$$f(r) = 0.017(3.3^r - 1) / [1 + 0.017(3.3^r - 1)] \qquad (12)$$

where

$$f = m / (M_u + m) \qquad (13)$$

is the rimed mass fraction, m is the mass of rime, and M_u is the mass of unrimed crystal. In the case of plate-like crystal, the change of the aspect ratio due to riming is proportional to 1/(1-f). If one assumes that the aspect ratio of unrimed plate-like crystal is 0.1, then riming with degree r = 4 would increase its aspect ratio by the factor of 3. Assuming that the density of unrimed and rimed crystals remains the same and equal to 0.5 g cm^{-3} this would result in the decrease of CDR from -11.5 dB to -15.4 dB which is quite significant change.

6 Conclusions

The methodology for measuring circular depolarization ratio (CDR) by dual-polarization radars with simultaneous transmission / reception along with traditionally measured Z_{DR}, ρ_{hv}, and Φ_{DP} in a single mode of operation has been suggested. This methodology implies the use of a high-power phase shifter to control system differential phase on transmission and special signal processing which eliminates detrimental impact of differential phase on the estimate of CDR.

Feasibility of the recommended approach has been demonstrated by retrieving CDR from other polarimetic moments and raw I and Q data as well as by implementing the scheme on the C-band radar with simultaneous transmission / reception of H and V waves.

As opposed to linear depolarization ratio LDR (which requires a special mode of operation), CDR is almost independent of hydrometeor orientation and is less affected by noise.

Three major challenging practical tasks can be addressed using CDR measurements: (1) detection of hail and determination of its size above the melting layer, (2) differentiating between various habits of ice aloft, and (3) quantification of riming which is associated with the presence of supercooled cloud water and signifies possible icing hazard to aircraft.

References

Al-Jumily, K., R. Charlton, and R. Humphries, 1991: Identification of rain and hail with circular polarization radar. *J. Appl. Meteor.*, **30**, 1075 – 1087.

Holt, A., V. Bringi, and D. Brunkow, 1999: A comparison between parameters obtained with the CSU-CHILL radar from simultaneous and switched transmission of vertical and horizontal polarization. Preprints, *29th Conf. on Radar Meteorol.,* Montreal, CA, 214 – 217.

Jameson, A., 1987: Relations among linear and circular polarization parameters measured in canted hydrometeors. *J. Atmos. Oceanic Technol*., **4**, 634 – 645.

Matrosov, S., 2004: Depolarization estimates from linear H and V measurements with weather radars operating in simultaneous transmission – simultaneous receiving mode. *J. Atmos. Oceanic Technol.*, **21**, 574 – 583.

Matrosov, S., Reinking, R. Kropfli, B. Martner, and B. Bartram, 2001: On the use of radar depolarization ratios for estimating shapes of ice hydrometeors in winter clouds. *J. Appl. Meteor.*, **40**, 479 – 490.

Matrosov, S., G. Mace, R. Marchand, M. Shupe, A. Hallar, and I. Mc Cubbin, 2012: Observations of ice crystal habits with a scanning polarimetric W-band radar at slant linear depolarization ratios mode. *J. Atmos. Oceanic Technol*., **29**, 989 – 1008.

Mosimann, L., E. Weingartner, and A. Waldvogel, 1994: An analysis of accreted drop sizes and mass of rimed snow crystals. *J. Atmos. Sci*., **51**, 1548 – 1558.

Ryzhkov, A., D. Zrnic, J. Hubbert, V. Bringi, J. Vivekanandan, E. Brandes, 2002: Polarimetric radar observations and interpretation of co-cross-polar correlation coefficients. *J. Atmos. Oceanic Technol.*, **19**, 340 - 354.

Ryzhkov, A., M. Kumjian, S. Ganson, and A. Khain, 2013a: Polarimetric radar characteristics of melting hail. Pt I: Theoretical simulations using spectral microphysical modeling. *J. Appl. Meteorol. Clim.,* **52,** 2849 – 2870.

Ryzhkov, A., M. Kumjian, S. Ganson, and P. Zhang, 2013b: Polarimetric radar characteristics of melting hail. Pt II: Practical implications. *J. Appl. Meteorol. Clim.,* **52**, 2871 – 2886.

Torlaschi, E., and A. Holt, 1993: Separation of propagation and backscattering effects in rain for circular polarization diversity S-band radars. *J. Atmos. Oceanic Technol.*, **10**, 465 – 477.

Torlaschi, E., and A. Holt, 1998: A comparison of different polarization schemes for the radar sensing of precipitation. *Radio Sci*., **33**, 1335 – 1352.

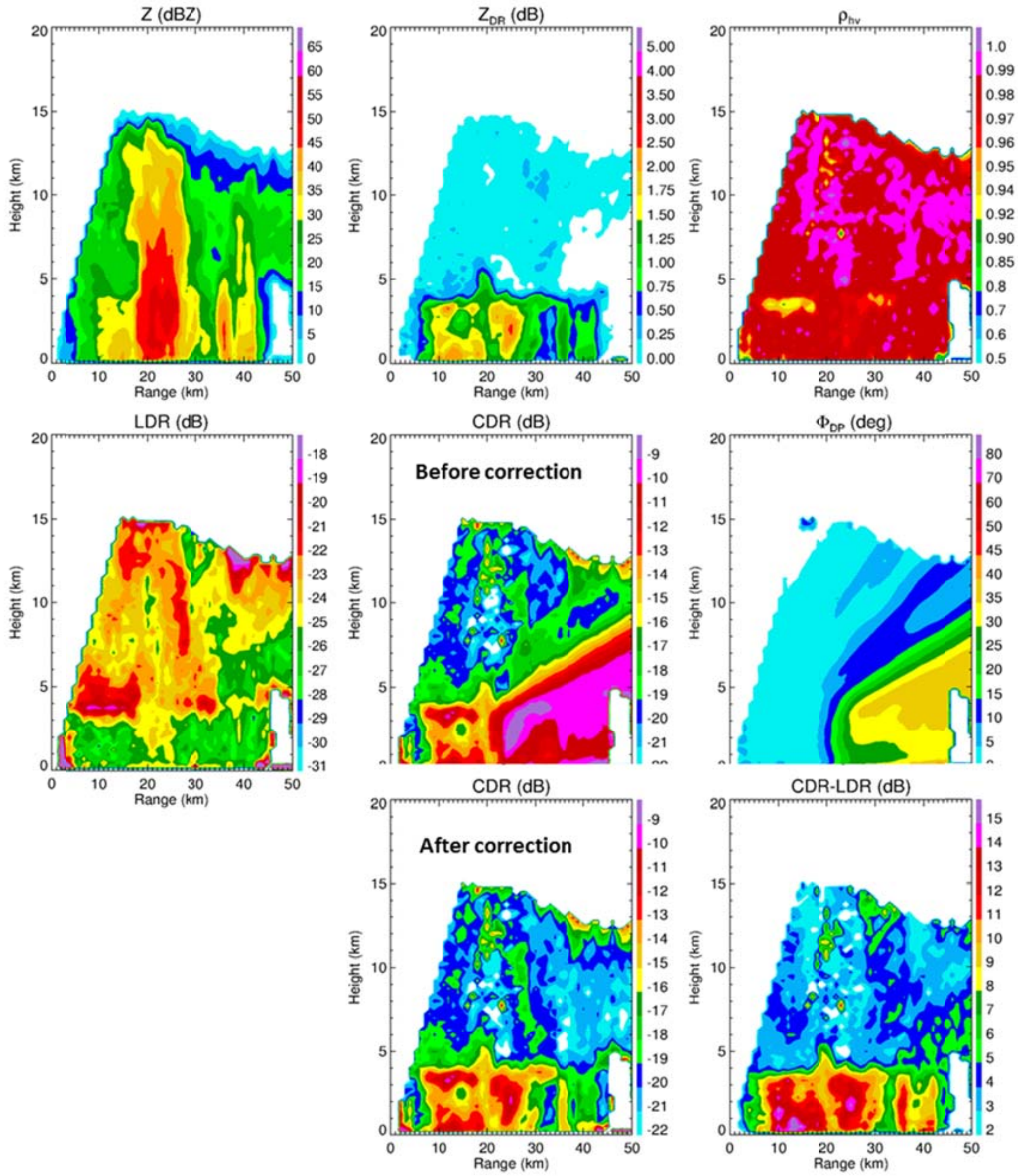

Fig. 1. Vertical cross-section of Z, Z_{DR}, ρ_{hv}, LDR, Φ_{DP}, CDR (before and after correction for propagation effects), and CDR - LDR for the case on 08/14/1998 at Az = 172.2°. The data are collected by the NCAR SPOL radar. CDR (before correction) is retrieved from the measured Z_{DR}, LDR, ρ_{hv}, and Φ_{DP} using Eq (2) assuming that system differential phase $\Phi_{DP}^{(t)}$ = 90°. CDR (after correction) is retrieved from Eq (5) with $\Phi_{DP}^{(t)}$ = 90°.

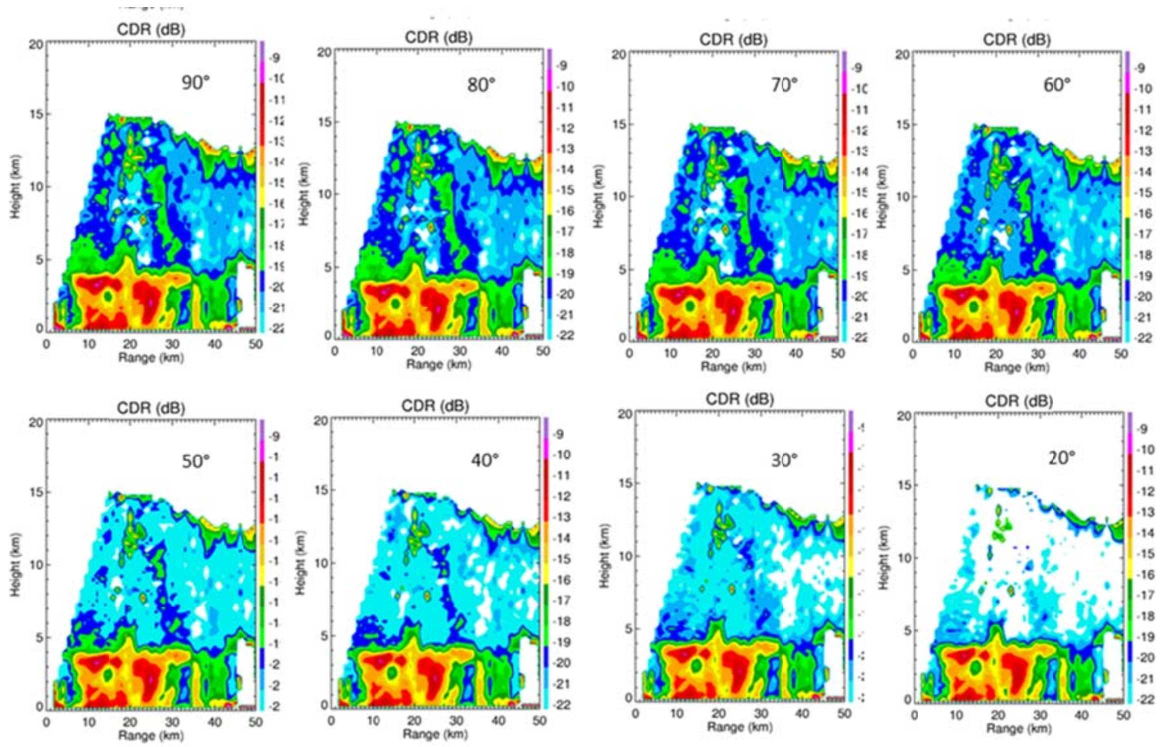

Fig. 2. Vertical cross-sections of estimated CDR for different values of system differential phase on transmission $\Phi_{DP}^{(t)}$ ranging from 90° (ideal setting) to 20° at the azimuth 172.2°.

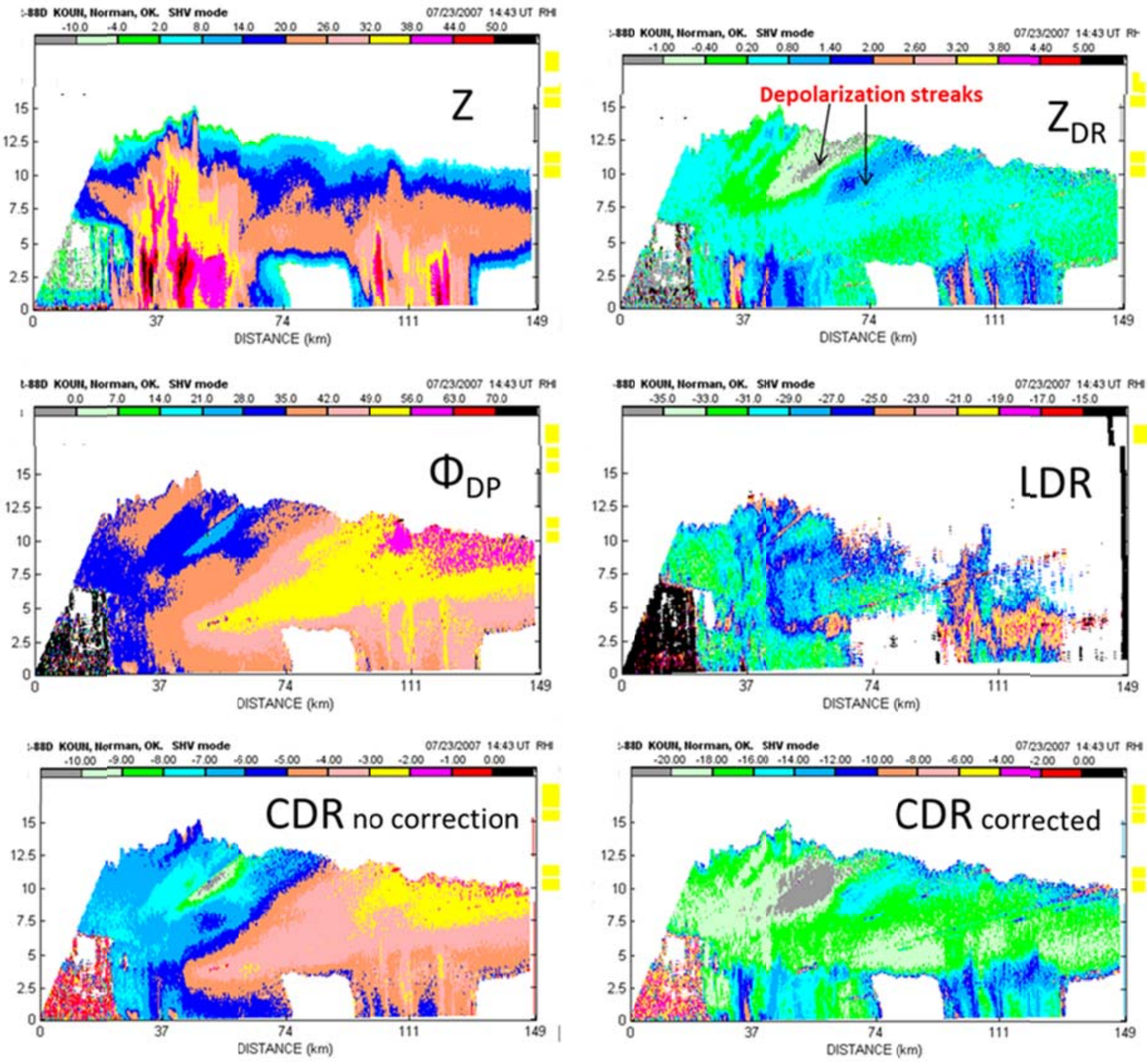

Fig.3. Composite RHI of Z, Z_{DR}, Φ_{DP}, LDR and CDR (with and without correction for propagation effects) retrieved from I and Q data collected by the KOUN WSR-88D radar on 07/03/2007. Z, Z_{DR}, Φ_{DP}, and CDR are measured in the SHV mode of operation (simultaneous transmission / reception of H and V waves). LDR is measured in the LDR mode when only the wave with horizontal polarization is transmitted.

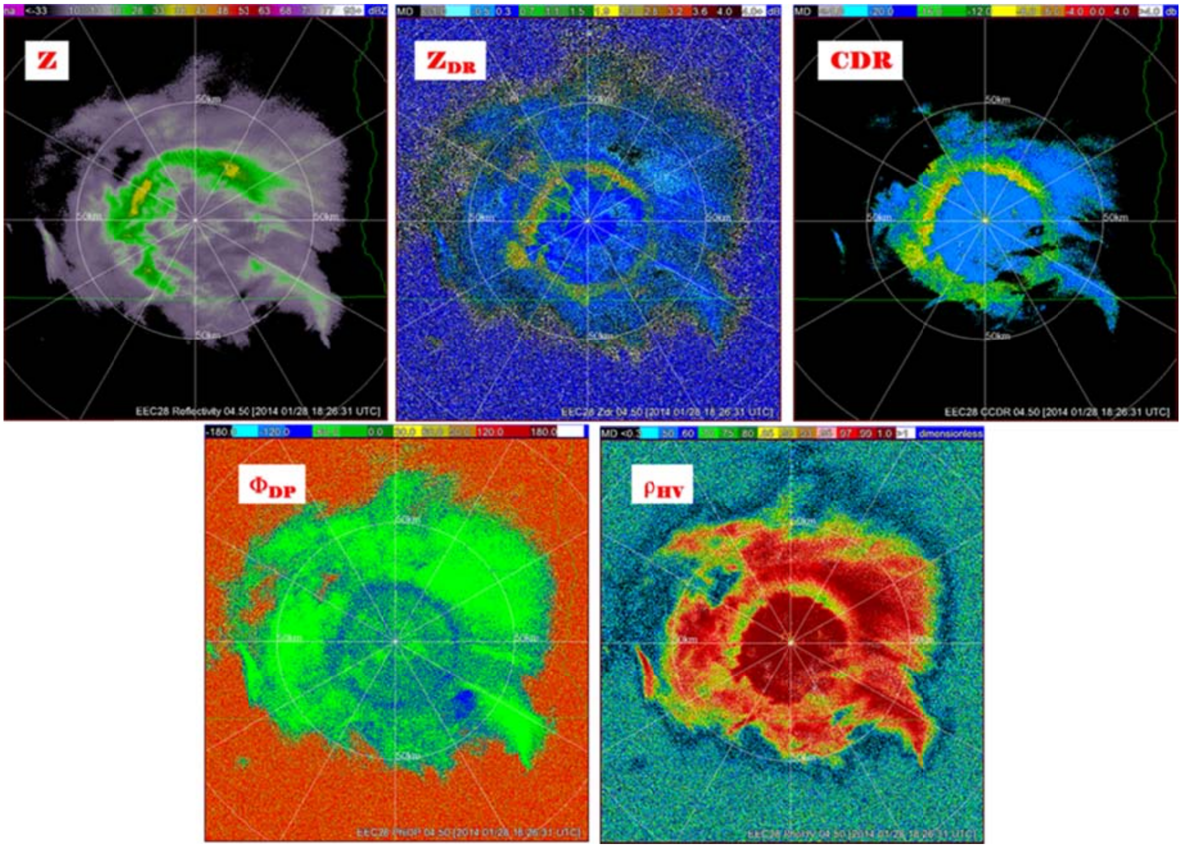

Fig. 4. Composite PPI of Z, Z_{DR}, CDR, Φ_{DP}, and ρ_{hv} at El = 4.5° measured by C-band radar at Enterprise, AL on 28 January 2014.

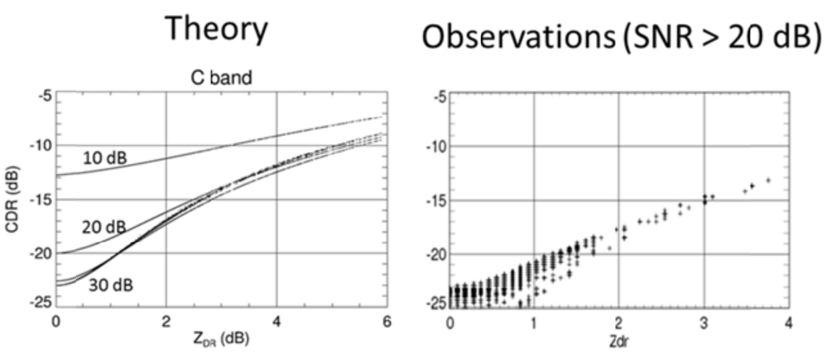

Fig. 5. (a) Theoretical dependencies of measured CDR on Z_{DR} in rain for different values of SNR; (b) scatterplot of measured CDR vs Z_{DR} in rain on 28 January 2014.

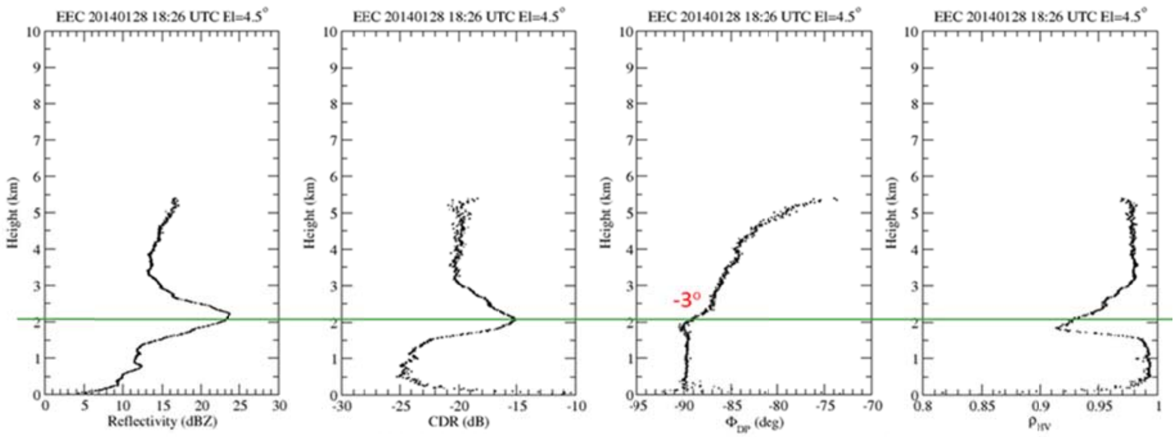

Fig. 6. Vertical profiles of Z, CDR, Φ_{DP}, and ρ_{hv} through the melting layer obtained by azimuthal averaging of the radar variables at El = 4.5° collected on 28 January 2014, 1826 UTC.